PHYSICAL REVIEW C VOLUME 4, NUMBER 6 DECEMBER 1971

Nuclear Structure of ^{23}Na: The ^{22}Ne(^{3}He, d) Reaction

J. R. Powers, H. T. Fortune, and R. Middleton
Department of Physics, University of Pennsylvania, Philadelphia, Pennsylvania 19104*

and

Ole Hansen
Department of Physics, University of Pennsylvania, Philadelphia, Pennsylvania 19104*
and Los Alamos Scientific Laboratory, University of California,† Los Alamos, New Mexico 87544

(Received 7 May 1971)

Using the ^{22}Ne(^{3}He, d)^{23}Na reaction at a bombarding energy of 15 MeV, excitation energies and angular distributions have been obtained for 96 levels below $E_x = 10.2$ MeV in ^{23}Na. Data were recorded in 3.75° steps in a multiangle spectrograph. Angular distributions were compared with distorted-wave Born-approximation predictions; values of transferred angular momentum and spectroscopic strength were extracted for 42 levels, including the three lowest $T = \frac{3}{2}$ states. An empirical forward-angle J dependence has been used to distinguish between $J_f^\pi = \frac{3}{2}^+$ and $\frac{5}{2}^+$ for $l_p = 2$ transfers. The summed $l_p = 0$ and $l_p = 2$ spectroscopic strengths agree with theoretical expectations. The results of the present investigation are combined with previous information and discussed in terms of the rotational model. The low-lying negative-parity states are examined in terms of their particle or hole character. The results for both positive- and negative-parity states suggest significant deviations from the predictions of a simple rotational model, even with band mixing.

I. INTRODUCTION

Considerable attention has been given in recent years to the nuclear structure of ^{23}Na, and its deformed character has been confirmed. Consensus appears to have been achieved regarding the spin-parity assignments of the levels below 5-MeV excitation energy. (See, e.g., Poletti, Becker, and McDonald,[1] and Durell *et al.*[2]) Overlapping tables of energy levels are reported by Dubois,[3] Hay and Kean,[4] and Endt and Van der Leun.[5] These provide a thorough listing of excitation energies through $E_x = 10$ MeV.

Dubois combined previous results (see Ref. 3 and references therein) with his own angular momentum transfers and stripping strengths obtained in the ^{22}Ne(^{3}He, d) reaction and constructed an outline of the low-lying rotational bands.[3] In the present experiment a larger energy interval is studied with better energy resolution. Angular momentum transfers are identified and spectroscopic information is extracted for a large number of new states. Gaps in previous analyses of the positive-parity bands are filled. New information is obtained for the negative-parity levels.

At the higher bombarding energy of the present work (15 MeV compared with 10 and 12 MeV for Dubois) the direct component of the reaction is more prominent. Previous results of (^{3}He, d) reactions in light nuclei have shown nondirect processes to be of importance at bombarding energies below 15 MeV.[6]

In Dubois's review of previous investigations,[3] Grubler and Rossel[7] are cited as suggesting a level observed at 7.72 ± 0.05 MeV in the ^{22}Ne(d, n) reaction as the lowest $T = \frac{3}{2}$ level in ^{23}Na – the analog of the ground state of ^{23}Ne. Dubois identified this with the level he observed at 7.890 ± 0.030 MeV. Using the ratio of the differential cross sections for (p, t) and (p, ^{3}He) reactions on ^{25}Mg, Hardy *et al.*[8] confirmed the assignment of $T = \frac{3}{2}$ for the sole strongly excited state in the region of 7.8 MeV. From a distorted-wave Born-approximation (DWBA) analysis[8] this level is assigned $J^\pi = \frac{5}{2}^+$. From their study of the ^{22}Ne(d, n)^{23}Na reaction, Mubarakmand and Macefield[9] suggested a $\frac{1}{2}^+$ level at 8.62 ± 0.03 MeV as the second $T = \frac{3}{2}$ level. These results will be compared with our data.

From the ^{24}Mg(^{3}He, $\alpha\gamma$)^{23}Mg reaction Dubois and Earwaker[10] found some of the low-lying levels in ^{23}Mg to have negative parity in disagreement with the positive parities suggested for the analog states in ^{23}Na.[5,11] The negative-parity assignments for the levels at 2.64, 3.68, and 3.95 MeV in ^{23}Na were made by Durell *et al.*[2] An open question at present is the degree to which these represent hole or particle states. While previous opinion[2,3,12] is in favor of interpreting these states in terms of a hole in Nilsson[13] level 4, the experimental evidence does not seem conclusive.

The results of the present experiment are compared with the predictions of the Nilsson model using both Woods-Saxon and harmonic-oscillator wave functions.

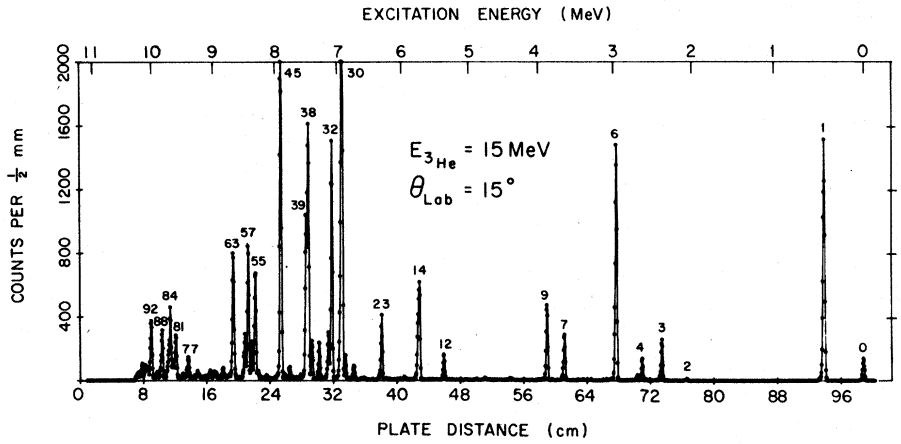

FIG. 1. Deuteron spectrum from the reaction ^{22}Ne(^{3}He,d)^{23}Na. Excitation energies for all groups observed are listed in Table I.

II. EXPERIMENTAL PROCEDURE

The experiment was performed with 15-MeV $^3He^{++}$ ions from the University of Pennsylvania tandem accelerator. The deuterons were detected in 25-μ NTA nuclear emulsion plates located at 7.5° intervals in a 24-angle multi-gap spectrograph. In the first exposure the most forward angle was 7.5°. A second exposure was obtained at a later date with the spectrograph rotated 3.75° toward larger angles. This gave, after normalization of the two runs, data from 7.5° in steps of 3.75°. Beam energies of 15.058 and 15.105 MeV were obtained for the two runs from detection of deuteron groups of known Q value. The total charge collected for each run was 2000 μC.

The target consisted of highly enriched ^{22}Ne gas (isotopic purity 99.8%)[14] which was recirculated through a gas cell with no entrance window.[15] The absence of an entrance window eliminated most of the beam-energy straggling and was the major factor in achieving 22-keV full width at half maximum (FWHM) energy resolution. The passage of the outgoing deuterons through a 520-μg/cm^2-thick Mylar exit window did not seriously affect the resolution. The entrance apertures to the gas cell were sufficiently narrow to maintain more than the 20-Torr pressure used in the experiment. The gas reservoir contained an absorber (Zeolite) which effectively prevented contamination by the usual sources – carbon, nitrogen, and oxygen – and no impurity groups were visible in the deuteron spectra. A deuteron spectrum obtained at a lab angle of 15° is displayed in Fig. 1.

The only serious experimental problem was a background of the order of about 2 counts per $\frac{1}{4}$-mm scan in the forward-angle spectra ($\theta_{lab} \leq 15°$). This background begins at the trailing edge of the large states and proceeds virtually undiminished for the length of the plate. In a separate 12 000-μC ^{22}Ne(^{3}He, d) exposure, group 3 (the first strongly populated state) had a peak yield at 7.5° of about 18 000 counts in a $\frac{1}{4}$-mm scan. Preceding the group the background was 0 to 2 counts per scan, but following the group it was 40–50 counts per scan. Scanning to the next intense group showed no significant decrease in the 40–50-count background, an effect that can be explained by energy losses incurred by deuterons which pass through small portions of the tantalum tubings that define the active target volume (Fig. 2). It should be noted that this background is negligible for all of the strong transitions, but at small angles it has a significant effect on the extraction of differential cross sections for the weaker states. The peak-fitting program AUTOFIT[16] was used to resolve the levels and sum the counts in each group.

III. EXPERIMENTAL RESULTS

The magnetic field (54 MHz) used in the present experiment is slightly higher than the highest field for which the magnet is linear, and hence the standard energy calibration was not strictly valid in the present experiment. A minor correction was made to the calibration assuming that previous excitation energies[3-5] were correct on the average. Excitation energies were compiled for 96 states below E_x = 10.218 MeV and are listed in Table I. Each excitation energy represents an average of the values determined at eight forward angles. The assigned errors are 5 keV or the standard deviation of the eight values, whichever was larger. For doublets, a minimum error of 10 keV was assigned, and for weakly populated members of partially resolved doublets, the assigned errors are even larger. The previously unreported levels 66(b), 66(c), 68(b), 80(b), and 86(b) were so weakly populated that their existence should be regarded as tentative, pending further investigation.

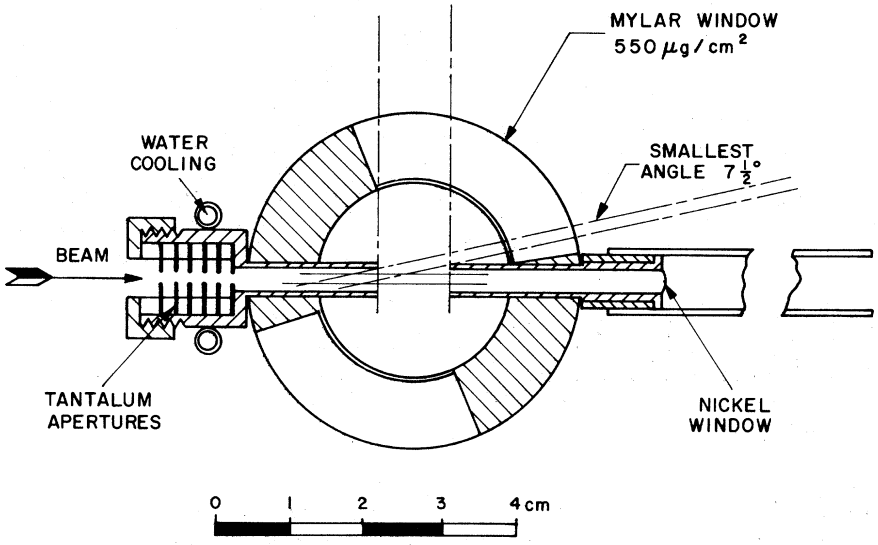

FIG. 2. Gas cell featuring no entrance window used in the present investigation.

The absolute cross-section scale was calculated from gas-cell and spectrograph geometry, total integrated charge, and gas cell pressure and may include an error of up to 10%. The experimental angular distributions are shown in Figs. 3–9. The error bars shown in the plots generally represent the larger of 5% or the statistical error. Larger error bars were assigned in the cases of a group falling on a plate cut, abnormally high counting rate, or questionable resolution by AUTOFIT. The estimated 10% uncertainty in the absolute cross-section scale is not included in these error bars.

IV. ANALYSIS

A. DWBA Calculations

Theoretical calculations of the angular distributions were performed within the usual DWBA formalism using the code DWUCK.[17] The potential well parameters for both the incoming and outgoing channels represent average sets which have given good results for other reactions in this mass and energy range.[18] These potentials are listed in Table II, along with the potential used to calculate the bound-state form factor.

The parameters used here improve significantly the prediction of the sharp decrease at forward angles for the $l_p = 2$ distributions as compared with the poorer fits of Dubois.[3] This is attributed principally to what is believed to be a more reasonable choice of V and r_0 in the outgoing channel and to the inclusion of spin-orbit coupling in all channels, including the bound states. The largest effect of spin-orbit coupling is in the bound state. The present parameters predict the secondary maxima of some $l_p = 0$ and 2 angular distributions lower than experiment. However, for the present data the

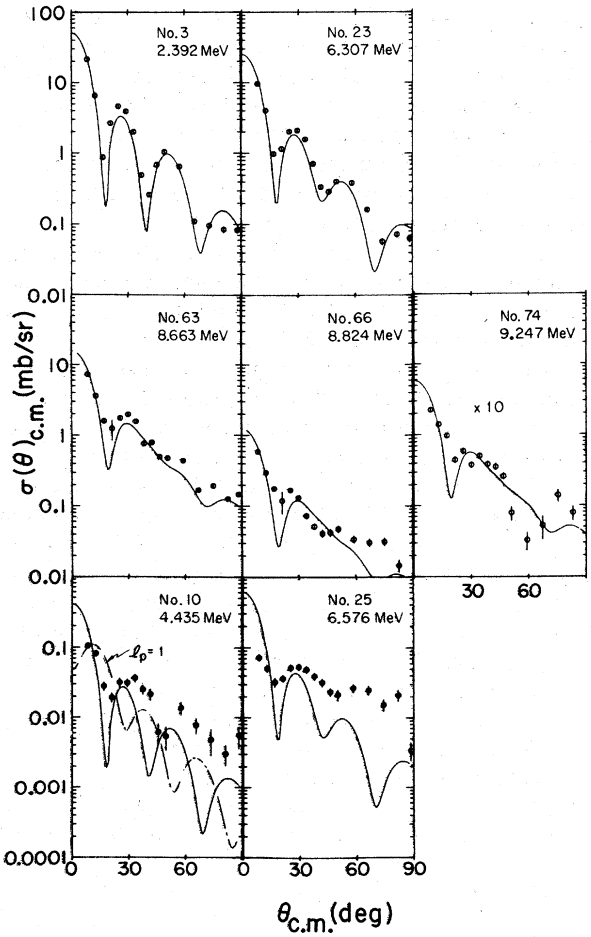

FIG. 3. Angular distributions of states showing $l_p = 0$ transitions. The solid lines represent the $l_p = 0$ DWBA predictions. The vertical scale is different for the weakly populated states Nos. 10 and 25.

TABLE I. ^{23}Na energy levels obtained from the ^{22}Ne(^{3}He, d) reaction.

Group	Energy (keV)	Previous Dubois	Previous Hay	Group	Energy (keV)	Previous Dubois	Previous Hay
0	g.s.	g.s.		54	8254 ± 5.0		8251
1	439 ± 8.8	439		55	8302 ± 5.0		8320
2	2078 ± 9.1	2080		56	8355 ± 5.1		8357
3	2392 ± 6.8	2391		57	8416 ± 5.0	8415	8413
4	2642 ± 9.5	2642		58	8468 ± 5.0		8469
5	2704 ± 6.3	2704		59	8498 ± 6.1		8501
6	2983 ± 7.0	2985		60	8555 ± 5.0		8555
7	3679 ± 7.0	3681		61	8602 ± 5.1		8605
8	3852 ± 8.0	3847	3850	62	8646 ± 10.0		8643
9	3918 ± 6.6	3917	3915	63	8663 ± 5.0	8659	
10	4435 ± 8.0	4430	4431	64	8721 ± 7.2		8715
11	4777 ± 7.6	4776	4775	65	8793 ± 5.3		8796
12	5378 ± 7.1	5379	5378	66(a)	8824 ± 5.7		8819
13	5536 ± 9.2	5537	5534	66(b)	(8862)		
14	5740 ± 7.8	5747	5738	66(c)	(8894)		
15	5762 ± 10.0		5762	67	8943 ± 5.4		8942
16	5776 ± 20.0		5782	68(a)	8972 ± 6.8		8965
17	5932 ± 6.6	5937	5934	68(b)	(9000)		
18	5968 ± 5.0	5970	5967	69	9036 ± 7.0		9037
19	6039 ± 6.6	6044	6042	70	9064 ± 5.0		9071
20	6116 ± 5.0		6115	71	9108 ± 6.0	Endt	9104
21	6193 ± 8.0	6192	6194	72	9167 ± 5.7		9170
22	6232 ± 9.6		6235	73	9210 ± 5.0		9210
23	6307 ± 5.3	6310	6304	74	9247 ± 5.6	9251	
24	6343 ± 9.0		6350	75	9282 ± 5.0		9280
25	6576 ± 5.0		6576	76	9320 ± 5.0		9320
26	6618 ± 5.4	6602	6619	77	9398 ± 5.0	9404	9400
27	6733 ± 5.0	6727	6731	78	9426 ± 5.9	9426	9425
28	6819 ± 5.4		6819	79	9482 ± 5.0	9486	9478
29	6866 ± 5.8		6865	80(a)	9540 ± 7.0		9537
30	6917 ± 5.3	6924	6914	80(b)	(9588)		
31	6943 ± 10.0		6940	81	9608 ± 6.7	9608	
32	7079 ± 6.1	7080	7070				9629
33	7130 ± 6.1		7125	82	9648 ± 7.0	9650	
34	7179 ± 6.9		7181		(Ref. a)	9653	
35	7275 ± 7.3	7277	7266		(Ref. a)	9672	9675
36	7386 ± 10.0		7386	83	9680 ± 6.9	9680	
37	7409 ± 10.0		7409	84	9704 ± 5.0	9700	
38	7451 ± 6.0		7446	85	9730 ± 5.0	9731	9732
39	7482 ± 8.7		7477	86(a)	9758 ± 5.0	9754	
40	7565 ± 5.4		7563	86(b)	(9780)		
41	7683 ± 5.8		7683	87	9818 ± 5.1	9814	9802
42	7725 ± 10.7		7721		(Ref. b)	9835	
43	7754 ± 6.2	7750	7745	88	9844 ± 5.5	9849	
44	7839 ± 10.0		7831	89	9887 ± 7.6	9889	
45	7889 ± 5.0	7890	7873	90	9925 ± 5.8	9914	
46	7960 ± 5.0		7961	91	9944 ± 10.0	9998	
47	7982 ± 12.0		7983	92	10018 ± 10.0	10014	
48	8063 ± 7.9		8057	93	10035 ± 10.0		
49	8101 ± 12.0		8100		(Ref. c)	10068	
50	8122 ± 6.7		8123	94	10077 ± 10.0	10073	
51	8149 ± 5.0		8151	95	10173 ± 10.0	10172	
52	8173 ± 6.7		8177	96	10218 ± 10.0	10227	
53	8220 ± 5.0		8220				

[a] 9648 certain doublet, possible triplet.
[b] 9844 probable doublet.
[c] 10077 probable doublet.

difference in spectroscopic factors calculated from the Dubois parameters and those used here is less than 2%.[19]

As is well known, the over-all slope of the calculated angular distributions is sensitive to the values of the absorptive potential. Decreasing W_D (the imaginary potential in the outgoing channel) according to $\Delta W_D/\Delta E_d = 0.5$ produced good agreement with the observed Q dependence of (^{3}He, d) angular distribution shapes. The effect of using $\Delta W_D/\Delta E_d > 0.8$ was tested in the region $E_x \approx 8$ MeV. With this larger value of $\Delta W_D/\Delta E_d$ a known $l_p = 2$ angular distribution was found to more closely resemble an $l_p = 3$ distribution. No ambiguity exists in identifying angular momentum transfers for the strongly populated states which possess definite stripping patterns, since there is a reasonable difference in the angular location of the points of inflection for the $l_p = 2$ and 3 curves. However, for the weak states these points of inflection may not be recognizable and some ambiguity between $l_p = 2$ and 3 may remain for the weak states. All calculations were done for $\Delta W_D/\Delta E_d = 0.5$.

Since DWUCK has no internal provision for calculating the form factor at energies at which the transferred proton is unbound, the DWBA calculations assumed a binding energy of 0.01 MeV for all levels above 8.792 MeV. Based on experience with other (^{3}He, d) reactions, this assumption should not significantly alter the shape of the DWBA distribution for states which are only slightly unbound. However, the true value of the transition strengths will become increasingly higher than those listed in Table III as the proton is increasingly unbound. It is now possible to do the DWBA calculations correctly for stripping to unbound states,[20] and calculations are in progress.

Spectroscopic factors were calculated from the relationship[21]

$$\sigma_{\text{exp}} = 4.42 \frac{2J_f + 1}{2J_i + 1} C^2 S \frac{\sigma_{\text{DWUCK}}}{2J_x + 1}.$$

The spectroscopic strengths are given in Table III

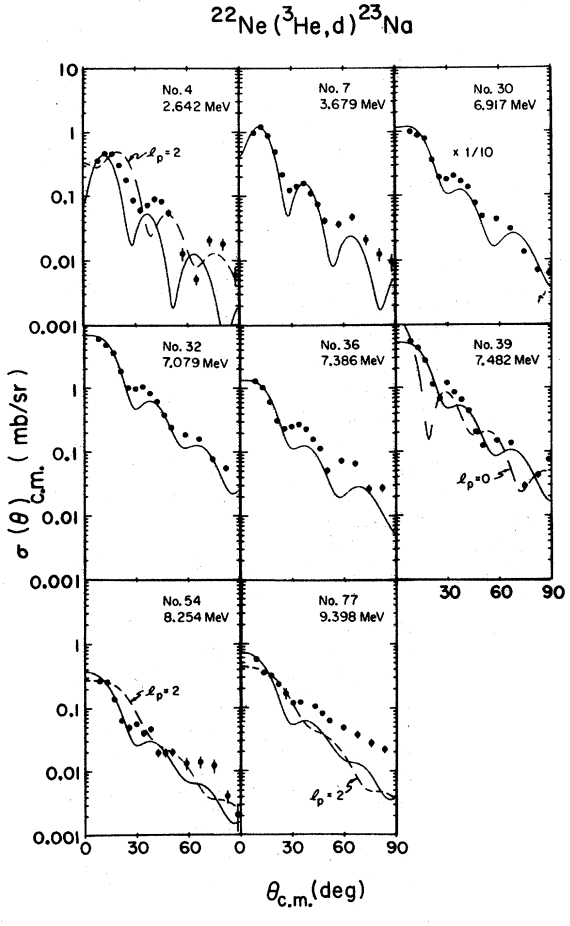

FIG. 4. Angular distributions of states showing $l_p = 1$ transitions. The solid lines represent the $l_p = 1$ DWBA predictions. Alternate $l_p = 0$ or $l_p = 2$ DWBA predictions are shown as a broken curve for some states.

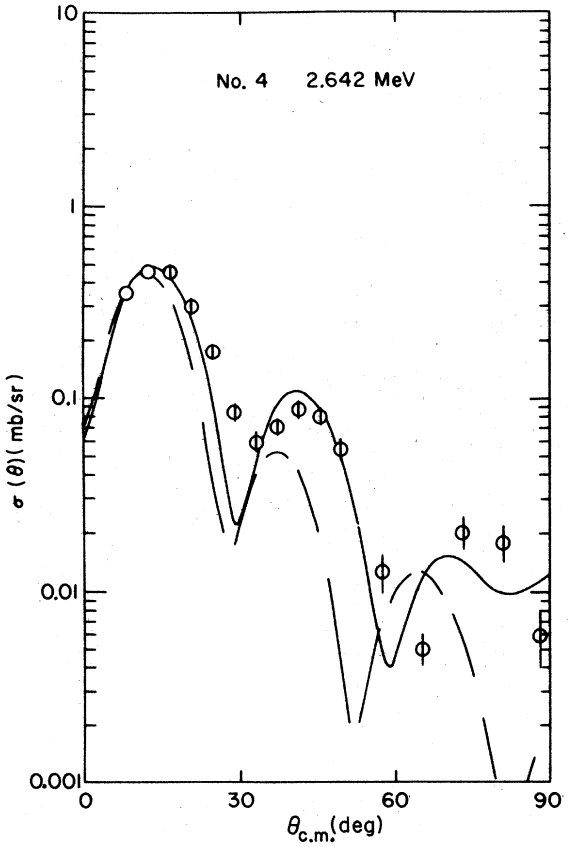

FIG. 5. The angular distribution of level 4 is shown with $l_p = 1$ DWBA calculations using $B_x = -22$ MeV (solid line) and $B_x = -6.15$ MeV (broken line).

TABLE II. Optical-model parameters used in DWBA calculations.

Channel	V_0 (MeV)	$r_0=r_{so}$ (fm)	$a_0=a_{so}$ (fm)	W (MeV)	W' (MeV)	r_0' (fm)	a' (fm)	V_{so} (MeV)	r_C (fm)	Reference
^{22}Ne+^{3}He	−177.0	1.138	0.7236	−13	0	1.602	0.769	−8.0	1.40	18
^{23}Na+d	−105.0	1.02	0.86	0	80 [a]	1.42	0.65	−6.0	1.30	18
^{22}Ne+p		1.26	0.60					$\lambda=25$		6

[a] $W'=4W_D$ and $W'=80-2.0E_x$.

in the form $(2J_f+1)C^2S$, since the final-state angular momentum and isospin are not certain in all cases. The quantity C is an isospin Clebsch-Gordan coefficient, $C=\langle T_i, t_x, T_{iz}, t_{xz} | T_f, T_{fz}\rangle$, where t_x is the isospin of the transferred particle. For the reaction ^{22}Ne(^{3}He, d)^{23}Na, the two possibilities are $C^2=\frac{2}{3}$ for $T_f=\frac{1}{2}$ and $C^2=\frac{1}{3}$ for $T_f=\frac{3}{2}$. Where significant, Table III incorporates results from other reactions.[22,23]

The DWBA calculations which were used to identify angular momentum transfer and to extract spectroscopic factors assumed the zero-range local (ZRL) potential option and were performed for lower cutoff radii $R_{co}=0$. The effects of finite-range nonlocal (FRNL) corrections and the effect of using a nonzero lower radial cutoff were investigated for $l_p=0$ and 2. In no case did a significant change in shape result. However, it can be seen from Table IV that the magnitude of the calculated cross sections were affected.

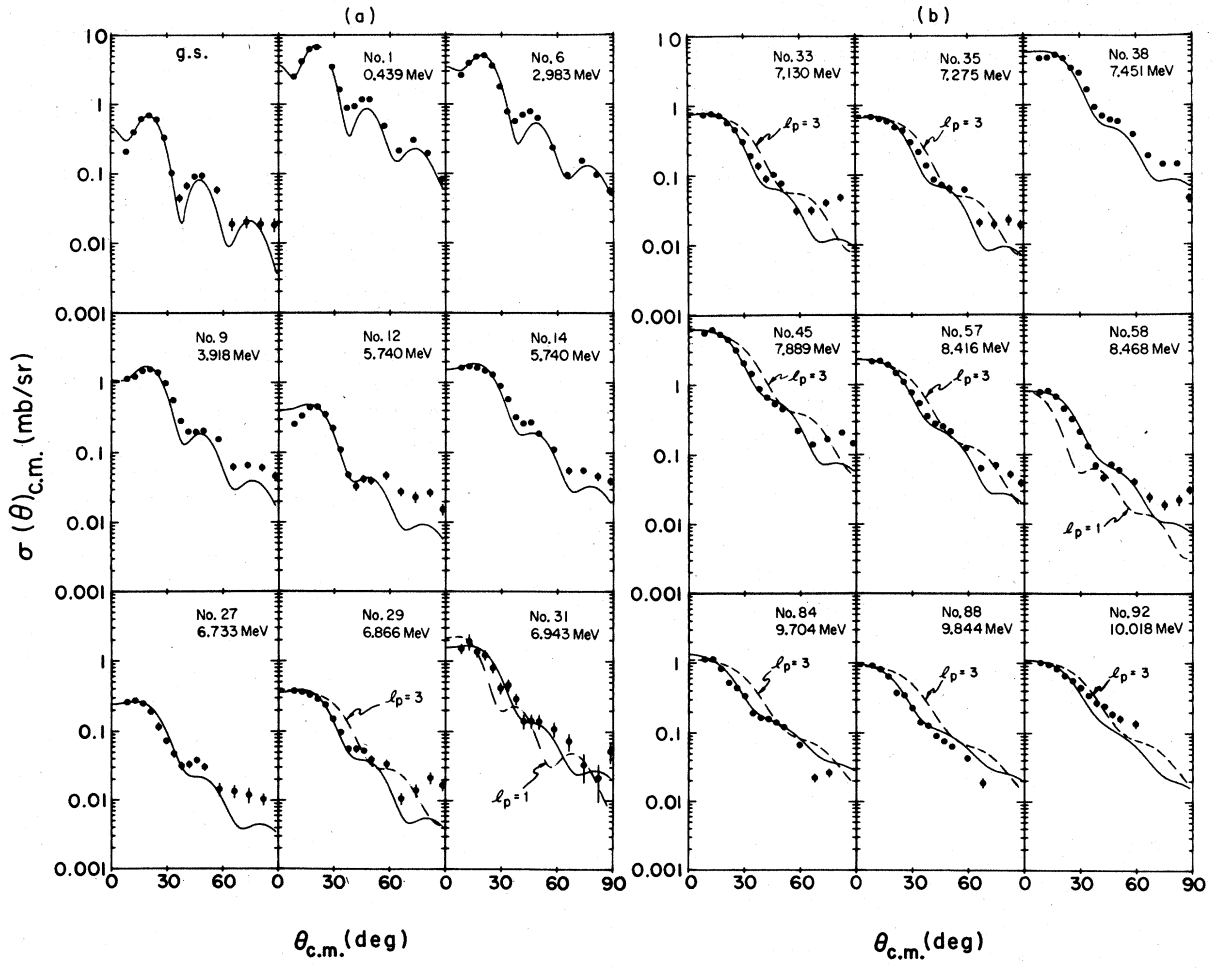

FIG. 6. Angular distributions of states showing $l_p=2$ transitions: (a) levels with $E_x<7$ MeV; (b) levels with $E_x>7$ MeV. DWBA calculations using $l_p=2$ (solid curves) and alternate $l_p=1$ or 3 (broken curves) are superimposed for certain states.

B. Discussion of l_p Assignments

1. $l_p = 0$

It may be seen from Fig. 3 that the angular distributions for levels 3, 23, 63, 66, and 74 are unambiguously characteristic of $l_p = 0$ transitions. The $l_p = 0$ assignments for levels 66 and 74 are new. Level 10 is very weakly populated and an $l_p = 0$ assignment cannot be made from the present data. However, level 10 appears[3] to be the mirror of the 4.355-MeV state of ^{23}Mg, a state which is strongly populated by $l_n = 0$ pickup in the reaction ^{24}Mg-(^{3}He, α)^{23}Mg.[10] Hence it seems probable that state 10 in ^{23}Na has $J^\pi = \frac{1}{2}^+$. The distribution for the transition to state 25 is similar to the one for state 10 and hence may possibly represent another weak $l_p = 0$ transition.

2. $l_p = 1$

Angular distributions characteristic of $l_p = 1$ are shown in Fig. 4. Firm $l_p = 1$ assignments can be made for transitions to levels 7, 30, 32, 36 + 37, and 39 in spite of the inferior quality of the fits at large angles. The DWBA curves shown were all calculated for $2p$ transfers; calculations for $1p$ transfer yield very similar shapes. However, the spectroscopic strengths calculated using a $1p$ transfer are approximately 2.6 times those using a $2p$ transfer for the same data.

Of particular interest are levels 30 and 39, members of previously unresolved doublets. These levels are separated by 26 and 31 keV from levels 31 and 38, respectively. The angular distributions of levels 31 and 38 are shown in Fig. 6. Dubois, in basing his assignments on the summed cross sections of the doublets, tentatively assigned $l_p = (1)$ to the 30, 31 pair and $l_p = (2)$ to the 38, 39 pair. These assignments agree with our results for the dominant member of each doublet. Level 30, the strong member of the lower doublet, is easily recognized as $l_p = 1$. However, since level 39 is the weaker component of the 7.5-MeV doublet, its $l_p = 1$ character was obscured in the earlier work[3] by the stronger member and the present $l_p = 1$ assignment to level 39 is therefore new. It was impossible to resolve levels 36 and 37 in the present work, and the distribution shown for level 36 is the sum of the cross sections of the two. The summed distribution appears to be characterized by $l_p = 1$.

The transitions to levels 54 and 77 are consistent with $l_p = 1$, but $l_p = 2$ cannot be ruled out. The two states are separated by 34 and 28 keV from levels 53 and 78, respectively.

The $l_p = 1$ fit to level 4 represents a special case. Consistently, in our data and in the data of Dubois, the data lie at larger angles than the distorted-wave curve. A similar effect has been observed in other data for single-particle-transfer reactions in this mass region.[24,25] Even though the effect is well established experimentally, there exists as yet no consistent theoretical interpretation. The effect appears in the angular distributions for stripping reactions to states that are predominantly of hole character and for pickup reactions to states that are predominantly of particle character. The common feature of such data is that the binding energy of the state is such that the separation-energy (SE) techniques of calculating bound-state form factors leads to unrealistically shallow (or deep) potentials for the bound-state well.

In all cases known to the present authors, it has been possible[26] to fit the data by using a bound-state

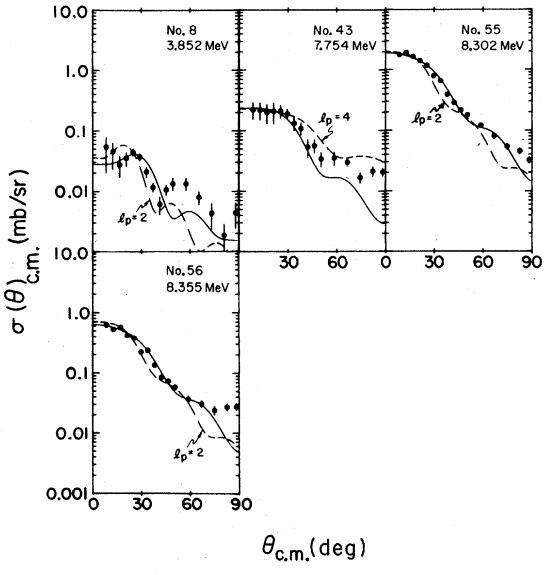

FIG. 7. Angular distributions for states showing $l_p = 3$ transition characteristics. The solid lines are $l_p = 3$ DWBA predictions. Alternate $l_p = 2$ or 4 DWBA calculations (broken curves) are given when appropriate.

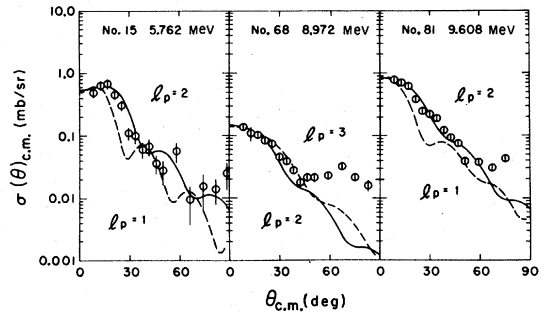

FIG. 8. Angular distributions of three states for which no preference between two l_p assignments can be made.

TABLE III. Angular momentum transfer and spectroscopic strengths for levels observed in the ^{22}Ne(^{3}He, d)^{23}Na reaction.

Group	Energy (keV)	J^π	l_p Present [a]	l_p Dubois	nl_j	$(2J+1)C^2S$
0	g.s.	$\frac{3}{2}^+$ [b]	2		$1d_{3/2}$	0.32
1	439	$\frac{5}{2}^+$ [b]	2		$1d_{5/2}$	2.10
2	2078	$\frac{7}{2}^+$ [b]	c		$1g_{7/2}$	≤0.18
3	2392	$\frac{1}{2}^+$ [b]	0	0	$2s_{1/2}$	0.50
4	2642	$\frac{1}{2}^-$ [b]	1	(1)	$1p_{1/2}$	0.043
5	2704	$\frac{9}{2}^+$ [b]			$1g_{9/2}$	≤0.36
6	2983	$\frac{3}{2}^+$ [b]	2	2	$1d_{3/2}$	1.28
7	3679	$\frac{3}{2}^-$ [b]	1	1	$1p_{3/2}$	0.076
8	3852	$(\frac{5}{2}^-)$ [b]	(3)	(3)	$1f_{5/2}$	0.033
9	3918	$\frac{5}{2}^+$ [b,d]	2	(2)	$1d_{5/2}$	0.27
10	4435	$\frac{1}{2}^+$	(0)	(0)	$2s_{1/2}$	0.006
11	4777	$(\frac{7}{2})^+$ [b,c]	c		$1g_{7/2}$	≤0.16
12	5378	$(\frac{5}{2})^+$ [b,d]	2	2	$1d_{5/2}$	0.074
13	5536		e			
14	5740	$(\frac{5}{2})^+$ [d]	2	(2)	$1d_{5/2}$	0.21
15	5762		2, (1)			
16	5776					
17	5932					
18	5968					
19	6039					
20	6119					
21	6193					
22	6232					
23	6307	$\frac{1}{2}^+$	0	0	$2s_{1/2}$	0.27
24	6343					
25	6576				$2s_{1/2}$	≤0.002
26	6618					
27	6733	$\frac{3}{2}$ $(\frac{5}{2})^+$ [d]	2	2	$1d_{3/2}$	0.030 [f]
28	6819					
29	6866	$(\frac{3}{2})\frac{5}{2}^+$ [d]	2		$1d_{5/2}$	0.032
30	6917	$(\frac{1}{2}, \frac{3}{2})^-$	1	(1)	$2p_{1/2}$	0.30
31	6943	$(\frac{3}{2}, \frac{5}{2}^+)$	(2)		$1d_{3/2}$	0.18
32	7079	$(\frac{1}{2}, \frac{3}{2})^-$	1	1	$2p_{1/2}$	0.17
33	7130	$(\frac{3}{2})\frac{5}{2}^+$ [d]	2		$1d_{5/2}$	0.065
34	7179					
35	7275		2 or 3		$1d_{5/2}$	0.058
					$1f_{5/2}$	0.24
36	7386	$(\frac{1}{2}, \frac{3}{2})^-$	1		$2p_{1/2}$	0.034 [g]
37	7409					

TABLE III *(Continued)*

Group	Energy (keV)	J^π	l_p Present [a]	l_p Dubois	nl_j	$(2J+1)C^2S$
38	7451	$(\frac{3}{2}, \frac{5}{2})^+$	2	(2)	$1d_{3/2}$	0.58
39	7482	$(\frac{1}{2}, \frac{3}{2})^-$	1		$2p_{1/2}$	0.15
40	7565				$1d_{5/2}$	≤0.01
41	7683				$1d_{5/2}$	≤0.01
42	7725					
43	7754	$(\frac{5}{2}, \frac{7}{2}^-)$	(3)		$1f_{5/2}$	0.084
44	7839					
45	7889	$(\frac{3}{2})\frac{5}{2}^+$	2	(2 or 3)	$1d_{5/2}$	0.46
46	7960					
47	7982					
48	8063					
49	8101					
50	8122					
51	8149					
52	8173					
53	8220					
54	8254	$(\frac{1}{2}, \frac{3}{2})^-$	(1)		$2p_{1/2}$	0.011
55	8302		3, (2)		$1f_{5/2}$	0.49
					$1d_{5/2}$	0.15
56	8355		3, (2)		$1f_{5/2}$	0.16
					$1d_{5/2}$	0.054
57	8416	$(\frac{3}{2}, \frac{5}{2})^+$	(2)		$1d_{5/2}$	0.18
58	8468	$(\frac{3}{2}, \frac{5}{2})^+$	2		$1d_{5/2}$	0.077
59	8498					
60	8555					
61	8602					
62	8646					
63	8663	$\frac{1}{2}^+$	0	0	$2s_{1/2}$	0.54
64	8721					
						h
66	8824	$\frac{1}{2}^+$	0			(0.05)
68	8943		2 or 3		$1d_{5/2}$	(0.013)
					$1f_{5/2}$	(0.030)
74	9247	$\frac{1}{2}^+$	0		$2s_{1/2}$	(0.032)
77	9398		1, (2)		$2p_{1/2}$	(0.039)
					$1d_{5/2}$	(0.032)
81	9608		1 or 2		$2p_{1/2}$	(0.077)
					$1d_{5/2}$	(0.11)
84	9704	$\frac{3}{2}(\frac{5}{2})^+$	(2)		$1d_{3/2}$	(0.27)

TABLE III *(Continued)*

Group	Energy (keV)	J^π	l_p Present [a]	l_p Dubois	nl_p	$(2J+1)C^2S$
88	9844	$\frac{3}{2}(\frac{5}{2})^+$	(2)		$1d_{3/2}$	(0.20)
92	10018	$(\frac{5}{2}, \frac{7}{2})$	2, (3)		$1d_{5/2}$	(0.18)
					$1f_{5/2}$	(0.40)

[a] Levels with insufficient stripping strength for l_p assignment are indicated by a blank in this column.
[b] Reference 1.
[c] Reference 22.
[d] Suggested by J dependence.
[e] $l=4$ from ^{23}Na$(p, p')^{23}$Na reaction. Reference 23.
[f] The value of $(2J+1)S$ for $J=l_p+\frac{1}{2}$ assumed in the DWBA is approximately 84, 76, and 61% of that calculated for $J=l_p-\frac{1}{2}$ in the case of $l_p=1$, 2, and 3, respectively.
[g] Includes level 37.
[h] The proton is unbound above $E_x=8792$ keV. The spectroscopic factors for the unbound states were calculated with $B_x=-10$ keV and are therefore uncertain to within 30%.

well whose depth reproduces the binding energy of known single-particle states rather than using the SE technique. Such a method is, of course, non-physical, since the tail of the bound-state wave function does not then have the correct asymptotic behavior. It would appear that a more physical solution to the problems lies in techniques of calculating form factors for two-particle–one-hole states (and one-particle–two-hole states) similar to that of Philpott.[27] Such a calculation for the 2.64-MeV state of ^{23}Na is shown as the solid line in Fig. 5.

3. $l_p=2$

The angular distributions characteristic of $l_p=2$ are shown in Fig. 6. The $l_p=2$ assignments for the ground state and levels 1, 6, 12, and 27 agree with previous firm assignments.[3] In addition, tentative $l_p=2$ assignments of Dubois[3] for levels 9, 14, and 38 are definitely confirmed in the present work. (The $l_p=2$ assignment for levels 14 and 38 became unambiguous as soon as the groups were resolved from the weaker members of their doublets.) Friesel, Lewis, and Miller[28] reported that level 9 is a doublet with 4-keV separation between the two states. The present angular distribution does not indicate the presence of components other than $l_p=2$. This state is discussed further in Sec. IV C.

TABLE IV. Ratios of maximum cross section to that calculated for ZRL with $R_{co}=0$.

Group	FRNL $R_{co}=0$	FRNL $R_{co}=3$	FRNL $R_{co}=6$	ZRL $R_{co}=3$	ZRL $R_{co}=6$
1 ($l_p=2$)	1.67	1.35	1.53	1.06	1.12
3 ($l_p=0$)	1.57	1.28	1.35	1.03	0.88

The transition to level 45 was identified as $l_p=2$ or 3 by Dubois but is positively identified here as $l_p=2$. This $l_p=2$ assignment is important, since it confirms the identification of level 45 as the lowest $T=\frac{3}{2}$ state (the ground state of ^{23}Ne has $J^\pi=\frac{5}{2}^+$).

The present $l_p=2$ assignments to levels 29, 33, and 58 are new. These levels were not identified in the report by Dubois[3]; however, the resolution of the present experiment enabled the extraction of angular distributions from these weakly populated states whose $l_p=2$ transition appears unambiguous.

The probable $l_p=2$ assignments to levels 31, 57, 84, 88, and 92 are also new. The angular distribution for level 31 shows that it has not been perfectly resolved from the stronger member of its doublet (level 30, $l_p=1$). Yet the fit for $l_p=2$ is sufficiently good on the average to make this tentative assignment.

As discussed in Sec. IV A, the differentiation between $l_p=2$ and 3 becomes increasingly more difficult as the excitation energy increases. For this reason, $l_p=3$ is not ruled out for level 57 and is as likely as $l_p=2$ for level 35. An extra problem is encountered for levels above 8.7-MeV excitation because of the high level density and the unbound nature of those states.

4. $l_p=3$

Angular distributions indicative of $l_p=3$ are shown in Fig. 7. The weak transition to level 8 does not permit an unambiguous $l_p=3$ assignment but the angular distribution is included here because of the known $J^\pi=\frac{5}{2}^-$ assignment to that state.[1] The $l_p=3$ assignment to the weakly populated states 43 and 56 are highly tentative. The $l_p=3$ assignment is less uncertain for level 55, which is more strongly populated.

5. *Ambiguous l_p Assignments*

Levels 15, 68, and 81 are shown separately in Fig. 8 because of major ambiguities in making an l_p assignment. Level 15, as plotted, is the sum of the levels listed in Table III as 15 and 16. The major contributor, level 15, is probably characterized by $l_p = 2$. Since there seems to be a minor $l_p = 1$ contribution in the angular distribution of the doublet, it is conceivable that level 16 has negative parity.

There is no basis of choice between $l_p = 2$ and 3 for level 68 due to its weak cross section. The angular distribution for level 81 appears to favor $l_p = 2$, even though the points of inflection are not well fitted. The possibility exists that this state is a doublet (see Table I).

The angular distributions for which there is no clearly discernible stripping pattern are shown in Fig. 9. The known $\frac{7}{2}^+$ and $\frac{9}{2}^+$ members of the ground-state rotational band (levels 2 and 5) are plotted with $l_p = 4$ DWBA curves. These clearly indicate that any $1g_{7/2}$ and $1g_{9/2}$ particle strength that

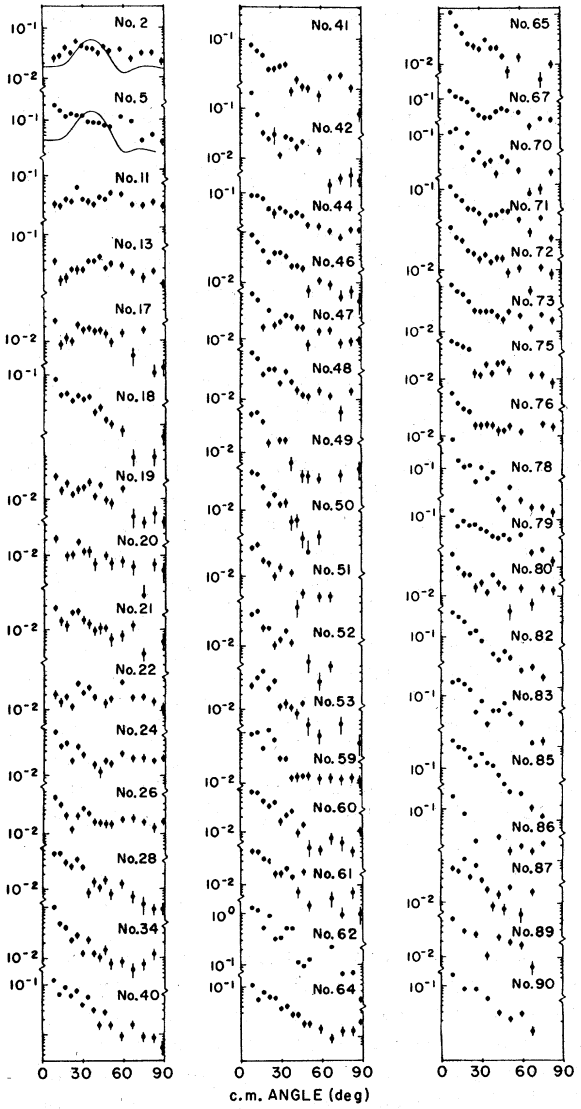

FIG. 9. Angular distributions for states not characteristic of pure $l_p = 0$, 1, 2, or 3 stripping.

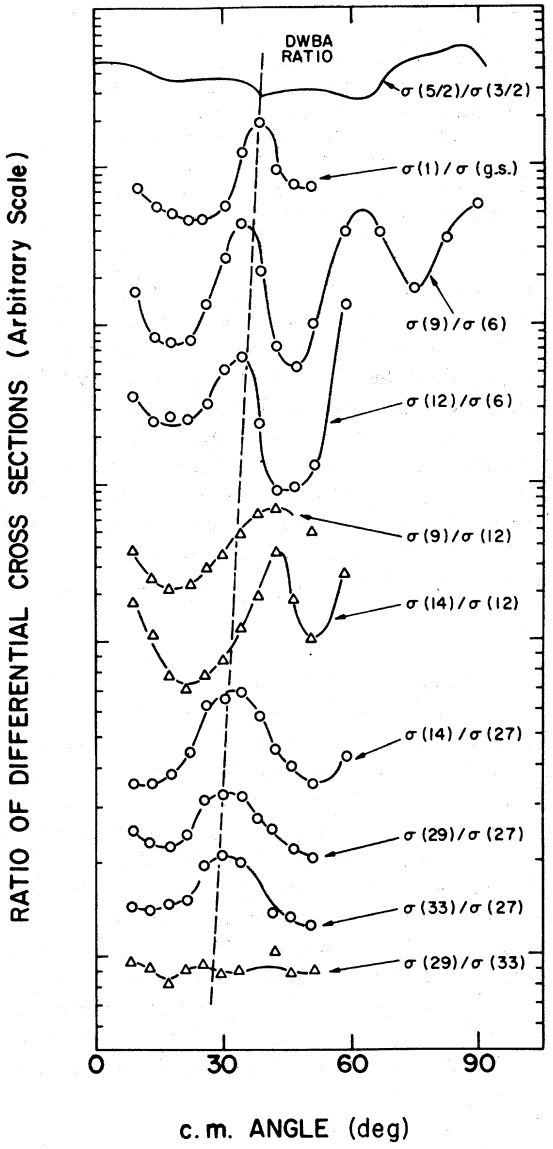

FIG. 10. Ratio of differential cross sections for selected states. Data shown with circles represent the ratio of the cross sections of a level assigned $J^\pi = \frac{5}{2}^+$ to a level assigned $J^\pi = \frac{3}{2}^+$. Triangles are used to show the ratio of two $J^\pi = \frac{5}{2}^+$ levels. The solid line at the top is the theoretical ratio of $J^\pi = \frac{5}{2}^+$ to $J^\pi = \frac{3}{2}^+$ cross sections. The dashed line drifting to the left highlights the Q-value shift of the maximum in the various ratios.

TABLE V. Summed transition strengths for $T=\frac{1}{2}$ positive-parity states in ^{23}Na.

Transition	$\sum(2J_f+1)C^2S$ Experimental	Nilsson [a]	Shell model [a]
$l_p=0$	0.86	0.95	1.33
$l_p=2$	6.03	6.38	6.00
Total	6.89	7.33	7.33

[a] The theoretical sums correspond to no core excitation in the ^{22}Ne ground state. They are calculated using the Nilsson wave functions of Chi ($\delta=0.3$) (Ref. 32) and the pure configuration shell model. The theoretical $l_p=0$ values will be slightly reduced if core excitation is introduced.

may exist at these excitation energies is small (see Table III).

C. J Dependence

Among the $l_p=2$ transitions, a significant difference is observed between the distributions for final state $J^\pi=\frac{5}{2}^+$ and $J^\pi=\frac{3}{2}^+$. The $\frac{5}{2}^+$ states have an appreciably flatter first maximum and a less steep slope leading to the first minimum. These differences are amplified when plotted as a ratio of cross sections for a $J^\pi=\frac{5}{2}^+$ level and a $J^\pi=\frac{3}{2}^+$ level. Such ratios for selected states are displayed in Fig. 10. The theoretical ratio shown in Fig. 10 was obtained by setting $J^\pi=\frac{5}{2}^+$ and $J^\pi=\frac{3}{2}^+$ in separate DWBA calculations for the ground state. It can be seen that this J dependence is not reflected in the theoretical DWBA distribution. Phenomenologically, however, the effect appears to be well established. (A similar effect has been noted for other sd-shell nuclei.[29]) Since the pattern is destroyed by any major nonstripping component, the ratios are not shown beyond an angle at which this component becomes significant.

The data presented in Fig. 10 for levels 6 and 9 led to an assignment[30] of $J^\pi=\frac{5}{2}^+$ for level 9, an assignment confirmed by Poletti, Becker, and McDonald.[1] Probable $J^\pi=\frac{5}{2}^+$ assignments for levels 12, 14, 29, and 33 and $J^\pi=\frac{3}{2}^+$ for level 27 are justified by good consistency between the ratios. It is noted that the first maximum in the ratio shifts toward forward angles with increasing excitation energy.

Also shown in Fig. 10 is the cross-section ratio for various states with the same J^π. The difference between these and the $\sigma(\frac{5}{2}^+)/\sigma(\frac{3}{2}^+)$ ratios support the above assignments. An attempt was made to extend this method to higher excitation energies but Q-value effects and less definitive resolution rendered the results inconclusive.

D. Spectroscopic-Factor Sum Rules

Disregarding possible core excitations, the ground state of ^{22}Ne has two protons (and hence 10 proton holes) in the sd shell. Thus, one should have

$$\sum_{\text{all } l_p=0 \text{ and } 2}(2J_f+1)C^2S_{lj}=10.$$

The experimental sum is 8.0, indicating that most of the available sd strength has been located.

The splitting of this strength between $T_<$ and $T_>$ states is predicted by the French and MacFarlane sum rules (see, e.g., the summary of Ref. 31). For a target having $T=1$, $J^\pi=0^+$

$$\sum(2J_f+1)C^2S_<=\langle p \text{ holes}\rangle-\tfrac{1}{3}\langle n \text{ holes}\rangle,$$

$$\sum(2J_f+1)C^2S_>=\tfrac{1}{3}\langle n \text{ holes}\rangle.$$

A comparison of experimental and theoretical summed $T_<$ strength is contained in Table V. Theoretical values are given for both the Nilsson model and the pure configuration shell model. The agreement between experiment and the predictions of the Nilsson model are good for both $l_p=0$ and $l_p=2$. Strong support for the Nilsson picture is found in the high $l_p=0$ shell-model prediction which is outside the expected uncertainties in experimental spectroscopic strengths. The extreme single-particle shell model does not account for the partial filling of the $2s_{1/2}$ level (Nilsson orbit 6) in the ^{22}Ne ground state. The uncertainties in the summed sd strength are larger than the expected core excitation, so that no quantitative statement regarding core excitation can be made from the summed positive-parity strength. Since only the first few $T=\frac{3}{2}$ states have been observed, the $T_>$ sum rule is obviously not exhausted.

V. DISCUSSION

A. Negative-Parity States

In the present work several negative-parity states have been identified for the first time. Figure 11 contains an experimental energy-level dia gram of the negative-parity states, together with two theoretical negative-parity spectra. The theoretical energies were calculated from the expression

$$E_{JK}=\epsilon_K+\frac{\hbar^2}{2I}[J(J+1)-2K^2+(-1)^{J+1/2}\delta_{K,1/2}(J+\tfrac{1}{2})a],$$

where J is the total angular momentum of the state, K is the spin projection on the symmetry axis, ϵ_K is the Nilsson single-particle energy, and a is the decoupling parameter

$$a=\sum_{lj}(-1)^{j-1/2}(j+\tfrac{1}{2})|c_{lj}|^2.$$

Here, c_{lj} is the amplitude of the shell-model

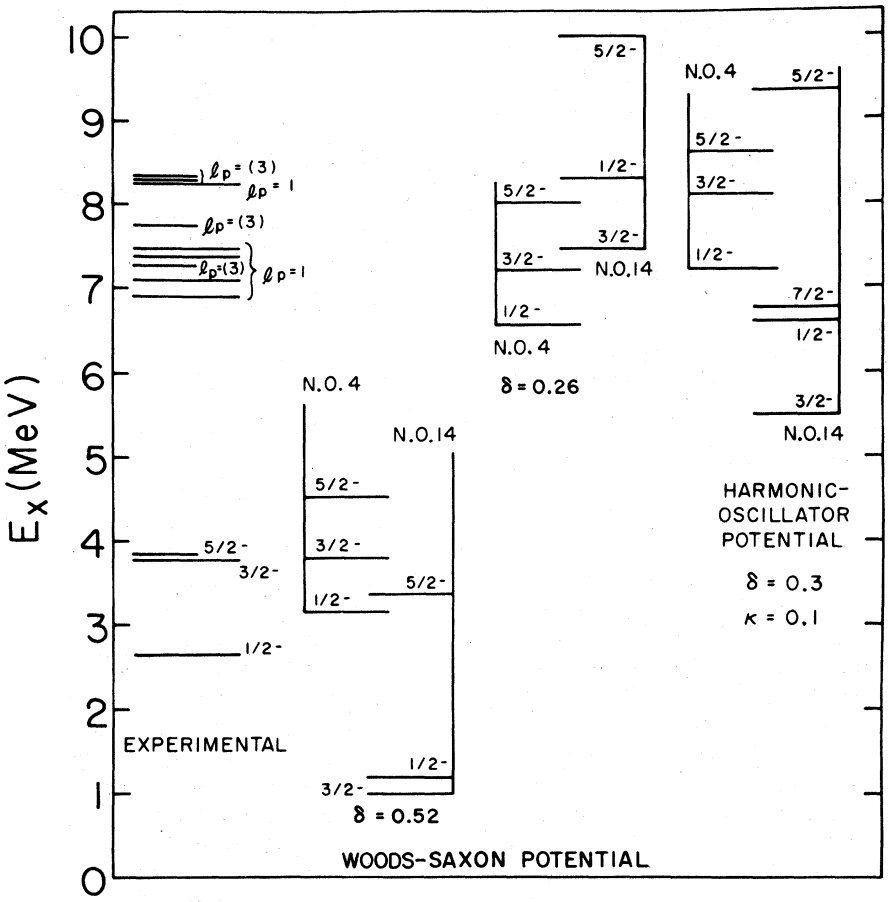

FIG. 11. Comparison of experimental and theoretical energy levels for the low-lying negative-parity states. The theoretical energy levels are discussed in the text.

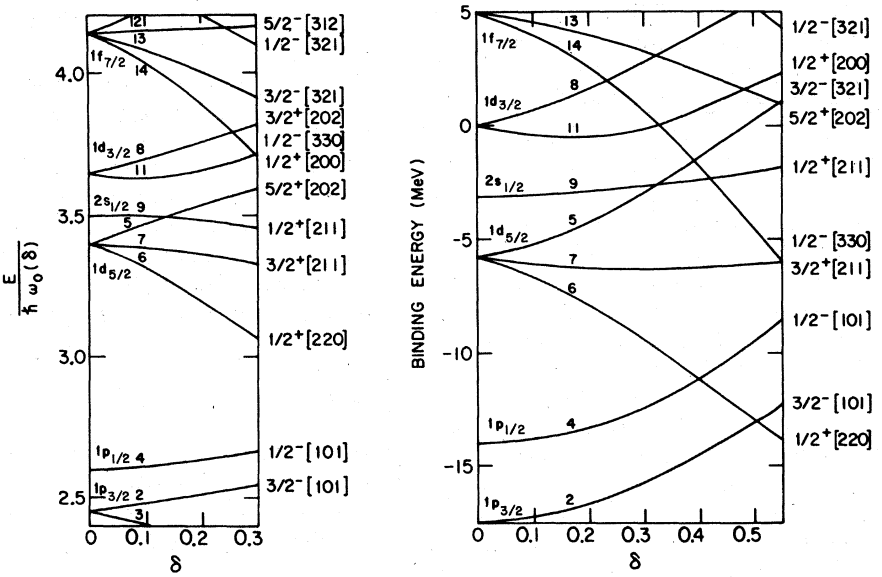

FIG. 12. Energy levels of the Nilsson levels (N.O.) as a function of deformation. The harmonic-oscillator wave functions (left) are based on the coefficients of Chi (Ref. 32). The deformed Woods-Saxon wave functions (right) were obtained with the coefficients of Ehrling and Wahlborn (Ref. 34).

TABLE VI. Experimental and theoretical transition strengths for groups 4, 7, and 8.

Group	J^π	Experimental $(2J+1)C^2S$ 1p	2p	1f	Theoretical[a] $(2J+1)C^2S$ Nilsson orbit 4[b] $\delta=0.3$	$\delta=0.52$	Nilsson orbit 14 $\delta=0.3$	$\delta=0.52$
4	$\frac{1}{2}^-$	0.043	0.017		0.043	0.038	0.104	0.182
7	$\frac{3}{2}^-$	0.076	0.030		0.009	0.012	0.061	0.670
8	$\frac{5}{2}^-$			0.033	0.000	0.000	0.079	0.4

[a] The theoretical values were calculated with $(2J+1)C^2S = 2|c_{lj}|^2$ where the c_{lj} were taken from $\delta=0.3$ harmonic-oscillator (Ref. 32) and $\delta=0.52$ Woods-Saxon (Ref. 34) wave functions.

[b] Assumes a (Nilsson level 4)$^{-2}$ impurity of 2.6% in the ground state of ^{22}Ne.

orbit lj in the intrinsic Nilsson wave function.

The calculations assumed the ground state contained one proton and two neutrons in the $K=\frac{3}{2}^+$ Nilsson orbit 7 (see Fig. 12). The two lowest negative-parity states which one can make in ^{23}Na correspond to elevating this odd proton to the $K=\frac{1}{2}^-$ Nilsson orbit 14 and to elevating a proton from the $K=\frac{1}{2}^-$ Nilsson orbit 4 to orbit 7. The first of these is a "particle" state and the second a "hole" state.

Calculations were performed for two different sets of Nilsson wave functions – harmonic-oscillator wave functions of Chi[32] and deformed Woods-Saxon wave functions.[33,34] The deformation parameter was taken to be $\delta=0.2$ and $\delta=0.3$ for Chi's wave functions and $\delta=0.26$ for the Woods-Saxon wave functions. In order to see what happens at large deformations, Woods-Saxon calculations were also performed for $\delta=0.52$, even though the deformation is expected to be closer to $\delta=0.3$.

It can be seen in Fig. 11 that neither calculation gives a good fit to experimental energy levels. The comparison of $l_p=1$ and $l_p=3$ spectroscopic strengths gives even poorer agreement, as can be seen from Table VI. The experimental $l_p=1$ spectroscopic factor obtained for level 4 under the assumption of 1p transfer can be made to agree with the predicted value if the ground state of ^{22}Ne is assumed to contain 2.6% (amplitude squared) impurity of two proton holes in the Nilsson orbit 4. However, the spectroscopic factors for the other levels are then in very poor agreement with the predictions. Even worse is the fact that, for most deformations, the lowest $\frac{1}{2}^-$ band comes from Nilsson orbit 14 rather than from 4. The only way to get the $\frac{1}{2}^-$ hole state, Nilsson orbit 4, below the $\frac{1}{2}^-$ particle state, Nilsson orbit 14, is to postulate a smaller deformation for the particle orbit than for the hole orbit. Some evidence exists for using different deformations for different bands, but in this mass region the evidence suggests that the hole orbit needs a smaller deformation, not a larger one.

The predicted spectroscopic strengths still bear little resemblance to experiment when different deformations are employed in order to better fit the observed energy levels. In addition, no improvement was obtained through band-mixing calculations performed for the $\frac{1}{2}^-$ members of the fp shell.

Only by using two different deformations as discussed above and by introducing *ad hoc* mixing between the particle and hole bands, is it possible to obtain fair agreement with the experimental data. We thus conclude that within the framework of the simple Nilsson model a description of the low-lying negative-parity states in ^{23}Na is not possible.

TABLE VII. Comparison of transitions strengths for selected $T=\frac{3}{2}$ candidates for the reactions ^{22}Ne$(d,p)^{23}$Ne and ^{22}Ne$(^3$He, $d)^{23}$Na.

nl_j	^{23}Ne E_x (MeV)	$(2J+1)S_{d,p}$ Ref. a	Ref. b	Ref. c	^{23}Na E_x (MeV)	E_x -7.89 (MeV)	$(2J+1)S_{^3\mathrm{He},d}$
$1d_{5/2}$	0.00	1.3	1.4	1.3	7.89	0.00	1.39
$2s_{1/2}$	1.02	1.4	0.78	1.2	8.66	0.77	1.62
$1d_{3/2}$	2.31	0.31			9.84	1.95	0.59[d]
$1d_{5/2}$	2.31	0.29	0.42	0.45	10.02	2.13	0.53

[a] Reference 35, $E_d=12.1$ MeV.

[b] Reference 36, $E_d=12.1$ MeV.

[c] Reference 37, $E_d=4.81$ MeV.

[d] This level has $(2J+1)S=0.46$ when the DWBA cross section is calculated for $1d_{5/2}$ transfer.

B. $T = \frac{3}{2}$ Levels

In order to confirm the $T = \frac{3}{2}$ assignments to level 45 and to locate the analog to the 1.02- and 2.31-MeV excited states in ^{23}Ne, a comparison of the transition strengths of the $(d, p)^{35-37}$ and $(^3\mathrm{He}, d)$ reactions has been made (Table VII.) The excellent agreement between the (d, p) strength to the ^{23}Ne ground state and the $(^3\mathrm{He}, d)$ strength to level 45 together with the present firm $l_p = 2$ assignment for the latter transition confirms its previous $T = \frac{3}{2}$ assignment[3,9] as the isobaric analog of the ^{23}Ne ground state.

The experimental evidence for recognizing level 63 (8.66 MeV) of ^{23}Na as the analog of the $J^\pi = \frac{1}{2}^+$ level at 1.02 MeV in ^{23}Ne is convincing. The value of $(2J+1)S$ for the $(^3\mathrm{He}, d)$ reaction is slightly higher than those listed for the (d, p) experiments. However, it is seen from Table III and Fig. 2 that in this excitation region there exists no other $l_p = 0$ transition with sufficient strength to correspond to the $T = \frac{3}{2}$ state. The value of $E_x - E_x$ (level 45) $= 0.77$ MeV compares well with the ^{23}Ne value of $E_x = 1.02$ MeV when the anticipated Thomas-Ehrman shift is taken into account.

The final determination of the analog to the 2.31-MeV ^{23}Ne level will be strongly influenced by the determination of the spin of that level. Lutz *et al.*[36] made a $J^\pi = \frac{5}{2}^+$ J-dependence assignment which, however, Howard, Pronko, and Whitten[35] dispute. In this region of the ^{23}Na spectrum the analog to the 2.31-MeV ^{23}Ne level can be narrowed to two candidates, levels 88 (9.84 MeV) and 92 (10.02 MeV). The strength for the transition to level 84 is too large and all other transitions are too weak. Based on the presently available evidence it is not possible to arrive at a clear choice between levels 88 and 92.

C. Positive-Parity Bands

Information obtained in the present work for the $l_p = 0$ and $l_p = 2$ transitions to $T = \frac{1}{2}$ final states is given in Table VIII. Also shown are the experi-

TABLE VIII. Experimental and theoretical transition strengths $(2J+1)C^2S$ in the reaction ^{22}Ne$(^3\mathrm{He}, d)^{23}$Na to members of rotational bands based on the $2s$-$1d$ Nilsson orbits (α).

Nilsson orbit α	Group	J^π	Energy (keV) Present	Energy (keV) Theoretical (Dubois [a])	Transition strength Experimental Present	Experimental Dubois	Theoretical [b] Unmixed	Theoretical [b] Mixed
7	0	$\frac{3}{2}^+$	0	0	0.32		0.082	0.161
	1	$\frac{5}{2}^+$	439	390	2.10		1.918	1.896
	2	$\frac{7}{2}^+$	2078	2150	≤0.18		0.	0.
	5	$\frac{9}{2}^+$	2704	2680	≤0.36		0.	0.
9	3	$\frac{1}{2}^+$	2392	2390	0.50	1.1	0.56	0.85
	6	$\frac{3}{2}^+$	2983	2970	1.28	1.3	0.92	1.45
	9	$\frac{5}{2}^+$	3918	3900	0.27	0.45	0.52	1.42
	11	$(\frac{7}{2})^+$	4777	4800	≤0.16	≤0.2	0.	0.
6	10	$\frac{1}{2}^+$	4435	4430	0.006			0.009
	12	$(\frac{5}{2})^+$	5378	5450	0.074			0.061
	31	$(\frac{3}{2})^+$	6943	6950	0.18			0.111
5	14	$(\frac{5}{2})^+$	5740	5900	0.21	≤0.55	2.00	1.44
11	23	$\frac{1}{2}^+$	6307	6310	0.27	0.75	0.96	0.84
	27	$(\frac{3}{2})^+$	6733	6630	0.03	0.04	0.96	1.60
	(40) [c]	$(\frac{5}{2})^+$	(7565)	7570	≤0.01		0.08	0.01
8	38	$(\frac{3}{2})^+$	7451	7470	0.58	≤1.1	1.92	0.62

[a] Based on RPC calculations by Dubois (Ref. 3) with $\kappa = 0.08$, $\mu = 0.0$, and $\delta = 0.2$ and where $\hbar^2/2I$ and E_α were treated as variables.

[b] The values for Nilsson orbits 9, 5, 11, and 8 are from Dubois (Ref. 3). Those for Nilsson orbits 7 and 6 assumed the parameters in Ref. a. The orbit 6 calculations assumed 1.8% core excitation (Nilsson orbit 6)$^{-2}$.

[c] Level 40 has $l_\alpha = 2$ from the ^{19}F$(^6$Li, $d)$ reaction (Ref. 22). Level 41 at 7683 keV also a possibility.

mental spectroscopic strengths from Dubois's work,[3] as well as the Coriolis coupling results from that work. The two sets of experimental strengths agree reasonably well, whereas some major differences between experiment and theory may be noted. Firstly, the ground-state transition (not observed in Ref. 3), is too strong – twice as strong as the prediction obtained after mixing.

Secondly, the strengths predicted for groups 14, 23, and 27 disagree strongly with observation. There seems to be no way of reconciling theory and experiment by reassigning states among the various rotational bands. An attempt was made to improve the agreement by performing Coriolis-coupling calculations at $\delta = 0.3$ and at larger deformation by simultaneously diagonalizing in the entire space covered by Table VIII (6 positive-parity bands). The results of this calculation showed discrepancies similar to those presented in Table VIII.

VI. CONCLUSIONS

The collective model, which has provided considerable insight into the structure of ^{23}Na, was seen to be in conflict with experimental results in two major instances, viz., in the identification of the negative-parity levels and the prediction of transition strengths for various positive-parity levels. Assumption of a uniform deformation for all of the bands in ^{23}Na, in particular for the negative-parity bands, seems very dubious in view of the data and analyses presented.

Subsequent experiments in this program will seek to eliminate as many of the current uncertainties as possible. Only then and after a more detailed calculation of the collective-model predictions can a fair judgment be made of its application to ^{23}Na.

ACKNOWLEDGMENTS

The authors would like to acknowledge Dr. K. Bethge for his assistance in the early phases of this work. The authors wish to thank Dr. J. Erskine and Dr. J. R. Comfort for allowing them to use the peak-fitting code AUTOFIT, Dr. S. Wahlborn and Dr. G. Ehrling for providing the finite-well Nilsson calculations, and Dr. M. Bunker and Dr. R. Storner for the use of their Coriolis-coupling code. The services of the computing centers of the University of Pennsylvania and at the Los Alamos Scientific Laboratory are gratefully acknowledged. The nuclear-emulsion plates were carefully scanned by Mrs. Joann Hoffman. Ole Hansen acknowledges travel support from NATO.

---

*Work supported in part by the National Science Foundation under contract with the University of Pennsylvania.

†Work supported in part by the U. S. Atomic Energy Commission under contract with the University of California.

[1]A. R. Poletti, J. A. Becker, and R. E. McDonald, Phys. Rev. C 2, 964 (1970).

[2]J. L. Durell, P. R. Alderson, D. C. Bailey, L. L. Green, M. W. Greene, A. N. James, and J. F. Sharpey-Schafer, Phys. Letters 29B, 100 (1969).

[3]J. Dubois, Nucl. Phys. A104, 657 (1967).

[4]H. J. Hay and D. C. Kean, Nucl. Phys. A98, 330 (1967).

[5]P. M. Endt and C. Van der Leun, Nucl. Phys. 34, 21 (1962).

[6]See, for example, H. T. Fortune, T. J. Gray, W. Trost, and N. R. Fletcher, Phys. Rev. 179, 1003 (1969), and references therein.

[7]W. Grubler and J. Rossel, Helv. Phys. Acta 34, 479 (1961).

[8]J. C. Hardy, H. Brunnader, J. Cerny, and J. Janecki, Phys. Rev. 183, 854 (1969).

[9]S. Mubarakmand and B. E. F. Macefield, Nucl. Phys. A98, 97 (1967).

[10]J. Dubois and L. G. Earwaker, Phys. Rev. 160, 925 (1967).

[11]A. B. Clegg and K. J. Foley, Phil. Mag. 7, 247 (1962).

[12]A. R. Poletti, A. D. W. Jones, J. A. Becker, R. E. McDonald, and R. W. Nightingale, Phys. Rev. 184, 1130 (1969).

[13]S. G. Nilsson, Kgl. Danske Videnskab. Selskab, Mat.-Fys. Medd. 29, No. 16 (1955).

[14]Mound Laboratory Analysis Report No. MDO 556, September 1968 (unpublished).

[15]R. Middleton, in *Proceedings of the International Conference on Nuclear Reactions Induced by Heavy Ions, Heidelberg, Germany, 15–18 July 1969,* edited by R. Bock and W. R. Hering (North-Holland Publishing Company, Amsterdam, The Netherlands, 1970), p. 263.

[16]Courtesy of J. Erskine and J. R. Comfort, Argonne National Laboratory, Argonne, Illinois.

[17]The distorted-wave code, courtesy of P. D. Kunz, University of Colorado.

[18]See, for example, H. T. Fortune, N. G. Puttaswamy, and J. L. Yntema, Phys. Rev. 185, 1546 (1969).

[19]The theoretical cross sections were calculated for both Dubois's and the current parameters using DWUCK (see Ref. 17).

[20]C. M. Vincent and H. T. Fortune, Phys. Rev. C 1, 769 (1970).

[21]R. H. Bassel, Phys. Rev. 149, 791 (1966).

[22]J. R. Powers, K. Bethge, H. T. Fortune, and R. Middleton, Bull. Am. Phys. Soc. 16, 36 (1971).

[23]G. M. Crawley, Ph.D. thesis, Princeton University, 1965 (unpublished).

[24]C. Schmidt and H. H. Duhm, Nucl. Phys. A155, 644 (1970).

[25]J. D. Garrett, R. Middleton, and H. T. Fortune, Phys. Rev. C 2, 1243 (1970).

[26]H. T. Fortune and J. R. Powers, to be published.
[27]R. J. Philpott, Phys. Rev. C 2, 1232 (1970). See also W. T. Pinkston, R. J. Philpott, and G. R. Satchler, Nucl. Phys. A125, 176 (1969).
[28]D. L. Friesel, T. Lewis, and W. C. Miller, Bull. Am. Phys. Soc. 15, 544 (1970).
[29]B. Mertens, C. Mayer-Böricke, and H. Kattenborn, Nucl. Phys. A158, 433 (1970).
[30]J. R. Powers, H. T. Fortune, O. Hansen, R. Middleton, Bull. Am. Phys. Soc. 15, 484 (1970).
[31]See, for example, J. P. Schiffer, in *Isospin in Nuclear Physics*, edited by D. H. Wilkinson (North-Holland Publishing Company, Amsterdam, The Netherlands, 1969), p. 665.
[32]B. E. Chi, Nucl. Phys. 83, 97 (1966).
[33]J. D. Garrett, R. Middleton, D. J. Pullen, S. A. Andersen, O. Nathan, and O. Hansen, Nucl. Phys. A164, 449 (1971).
[34]G. Ehrling and S. Wahlborn, private communication,
[35]A. J. Howard, J. G. Pronko, and C. A. Whitten, Jr., Nucl. Phys. A152, 317 (1970).
[36]H. F. Lutz *et al.*, Nucl. Phys. A95, 591 (1967).
[37]H. Nann *et al.*, Z. Physik 218, 190 (1969).

PHYSICAL REVIEW C VOLUME 4, NUMBER 6 DECEMBER 1971

Properties of Levels in Cl^{34}

A. K. Hyder, Jr.,* and Gale I. Harris
Aerospace Research Laboratories, Wright-Patterson Air Force Base, Ohio 45433

(Received 28 July 1971)

22 levels of Cl^{34} below $E_x = 4.7$ MeV are populated by the γ-ray decay of the three resonances at $E_p = 1058$, 1098, and 1121 keV in the reaction $S^{33}(p,\gamma)Cl^{34}$. These resonances, selected for study because of their dominant modes of γ decay to levels above 2.7 MeV for which limited prior data exist, were investigated with an 80-cm^3 Ge(Li) detector, and with Ge(Li)-NaI coincidence and angular-correlation techniques. The results obtained for levels below 2.3 MeV are in general agreement with other recent work. A new result is a probable $J = 3$ assignment for the 2.180-MeV level. For higher-lying levels, γ-ray decay schemes and excitation energies with errors in the range from ±0.3 to ±2.3 keV were determined for 14 bound states in the range $2.3 < E_x < 4.7$ MeV and the three resonance levels. The reaction Q value was determined with the result $Q = 5139.9 \pm 0.9$ keV. The following J^π assignments (energies in MeV) result from the combination of the present work with a recent $S^{33}(He^3,d)Cl^{34}$ study: 2.72, 2^-; 3.55, 3^-; 3.60, $4^{(-)}$; 3.63, 5^-; 3.77, 1^-; 3.98, 3^-; 4.08, 4^-; 4.14, 2; 4.35, probably 1^-; 4.42, 1, 2, or 3; 4.51, probably 2^-; and 4.64, 2, 1, or 3. The resonance level assignments are $J^\pi(1058) = 3^{(-)}$, $J^\pi(1098) = 4^{(-)}$, and $J^\pi(1121) = 1^-$. It is shown that the three resonances are probably each odd-parity $T = 1$ levels. The probable shell-model configurations of some of the odd-parity levels are discussed.

INTRODUCTION

Very little experimental information on properties of energy levels of Cl^{34} was available until the marked increase in experimental interest which has occurred during the past two years. The theoretical importance of this self-conjugate odd-odd nucleus to an understanding of properties in the upper $2s$-$1d$ shell has been matched until recently by experimental difficulties associated with the relatively high level density. Most of this recent work has dealt with properties of levels below 3-MeV excitation. These studies include: the $S^{33}(p,\gamma)Cl^{34}$ decay-scheme and angular-correlation work by Graber and Harris;[1] the $S^{32}(He^3,p\gamma)Cl^{34}$ work from which branching ratios, spins and parities, and lifetimes have been obtained by Sykes[2] and by Brandolini, Engmann, and Signorini;[3] and accurate level energy measurements by Snover *et al.*[4] With this work, much detailed information including spin and parity assignments for all of the lowest six levels is now available.

Some progress has also been made in the determination of properties of higher-lying levels. Graber and Harris[1] examined several resonances in the reaction $S^{33}(p,\gamma)Cl^{34}$ with a 40-cm^3 Ge(Li) detector with considerable improvement over the results of older NaI(Tl) work.[5] Revised decay schemes for six resonance levels between $E_p = 1050$ and 1270 keV, and for 11 bound states below $E_x = 4$ MeV, were obtained. Unique spin assignments for two of the resonance levels and for the level at 2.376 MeV ($J = 4$) were obtained by $(p,\gamma\gamma)$ angular-correlation measurements. From another recent $S^{32}(He^3,p\gamma)Cl^{34}$ investigation, DeLuca, Lawson, and Chagnon[6] report $J = 1$ for the 2.581- and 3.126-MeV levels and $J = 2$ for the 2.722-MeV level. In older work, Dong-Hyok[7] studied the reaction S^{32}-